Land use transition and ecological consequences: a spatiotemporal analysis in south-eastern Bangladesh

Md. Riyadul Haque[1], Muhammad Moniruzzaman[1], Arman[1], Md. Rakibul Hasan[1], Tuhin Lat[1], Nasima Kabir[2], Md. Jahangir Sarker[3], Leonard Tijing[4], Ho Kyong Shon[4], Daniel A. Ayejoto[5], Mohd Yawar Ali Khan[6], Mohammad Mahbub Kabir[1,4,]*

[1]Department of Environmental Science and Disaster Management, Noakhali Science and Technology University, Noakhali-3814, Bangladesh.

[2]Department of Zoology, Faculty of Life and Earth Science, Jagannath University, Dhaka 1100, Bangladesh.

[3]Department of Fisheries and Marine Science, Noakhali Science and Technology University, Noakhali 3814, Bangladesh.

[4]School of Civil and Environmental Engineering, Faculty of Engineering and IT, University of Technology Sydney, P.O. Box 123, Broadway, NSW 2007, Australia.

[5]Department of Environmental and Sustainability Sciences, Texas Christian University, Fort Worth, TX, USA

[6]Department of Hydrogeology, Faculty of Earth Sciences, King Abdulaziz University, Jeddah 21589, Saudi Arabia

***Correspondence: Mohammad Mahbub Kabir**

Email: Mohammadmahbub.Kabir@student.uts.edu.au

Telephone: +61 451313534

School of Civil and Environmental Engineering, Faculty of Engineering and IT, University of Technology Sydney, P.O. Box 123, Broadway, NSW 2007, Australia.

Abstract

Urban and economic growth around the world have rapidly degraded the ecosystem and environmental quality. Chattogram, a renowned city in Bangladesh known for its scenic environment, has experienced significant urban growth, which has degraded the environmental and ecological quality to the greatest extent. To investigate this issue, we assessed the Chattogram Metropolitan Area (CMA)'s ecological quality using the remote sensing-based ecological index (RSEI), incorporating four ecological indices such as heat index (LST), wetness (WET), dryness (NDBSI), and vegetation index (NDVI) through principal component analysis (PCA) and random forest (RF) model to analyze land use transitions (LUTs) using an advanced google earth engine (GEE). The PCA1 accounted for 80% of the dataset, delving into the highly significant features. Land use and land cover classes (LULCs) showed a gradual expansion of urban areas over the last two decades, indicating socio-economic progress. The urban area expanded from 34.08 km² in 2003 to 101.99 km² in 2023, an increase of 67.91 km² over 20 years, with an annual expansion rate of 2.34 km²/year. The RSEI values remained consistently >0.6, indicating good ecological levels, primarily due to sustainable urban planning. RSEI negatively correlated with LST and NDBSI, suggesting a detrimental influence, particularly in urban and economic zones. Conversely, the NDVI and WET indices showed a positive correlation, indicating a constructive impact on the local ecological landscape. This study will assist policymakers in formulating strategies for ecological conservation to achieve sustainable development goals (SDGs) and implement the Chattogram Metropolitan Master Plan (2020-2041).

Keywords: *Bangladesh, degradation, ecology, GIS, modelling, RSEI, urban growth.*

1. Introduction

Land is the fundamental component of Earth, playing a crucial role in maintaining ecological processes and developing terrestrial ecosystems, which encompass complex interactions between living organisms and their environment (Ma and Zhang 2023; McCourt *et al.,* 2023; Wei *et al.,* 2023). Ecosystem services play a significant role in the well-being, socio-economic and environmental progress of humans (Hariram *et al.,* 2023; Sangha *et al.,* 2022). However, human activities have drastically destroyed the suitable land use patterns, known as land use transitions (LUTs), resulting in significant impacts on ecosystem services (Yin *et al.,* 2020). As a result, critical ecological zones, such as vegetation and water bodies, have experienced

progressive depletion and fragmentation (Tolessa *et al.,* 2017). In recent years, urban expansion has changed land use patterns and structures (Long *et al.,* 2021) and led to various ecological issues, such as air pollution, deteriorating soil quality, an increased urban heat island, and a loss of biodiversity (Ullah *et al.,* 2022). From 1997 to 2011, estimates of the projected annual loss in ecosystem service value (ESV) due to changes in land use ranged from 4.3 to 20.2 trillion USD globally (Costanza *et al.,* 2014; Yin *et al.,* 2020). Investigating, analyzing, and comprehending the processes of LULC is imperative for devising solutions to achieve a sustainable ecosystem (Airiken *et al.,* 2022; Mao *et al.,* 2023). Numerous researchers have employed various remote sensing indices to evaluate diverse ecosystems, including urban areas, forests, grasslands, and watersheds. The normalized difference vegetation index (NDVI) evaluates changes in forest ecosystems (Prăvălie *et al.,* 2022) while the normalized difference impervious surface index (NDISI) assesses urban ecological environments (Li *et al.,* 2021). The chlorophyll-a and suspended-solid indices analyze water quality, whereas land surface temperature (LST) assesses the influence of urban heat islands (Sekertekin and Zadbagher, 2021). Two primary ecological indicators, the ecological index (EI) (Karbalaei Saleh *et al.,* 2021) and the RSEI (Yuan *et al.,* 2021), are utilized to evaluate regional ecological conditions, whereas RSEI is superior to EI, demonstrating greater effectiveness in monitoring eco-environmental quality (EEQ) (Mao *et al.,* 2023). RSEI, which is based solely on remote sensing, incorporates four key ecological indicators: heat index, wetness, vegetation index, and dryness. Numerous studies currently assess the ecological environment at various levels, ranging from global to intercontinental (Lu *et al.,* 2019), national (Liao and Jiang, 2020), urban agglomeration (Ji *et al.,* 2020), and city levels (Lu *et al.,* 2023).

Bangladesh is a developing country with a substantial population (Rahman *et al.,* 2023; Soma *et al.,* 2023), which often leads to alterations in the natural landscape or land use (Rahaman *et al.,* 2023). Chattogram, situated in southeastern coastal Bangladesh, stands as one of the nation's most renowned and industrially productive cities, often referred to as the commercial capital and the gateway to Bangladesh (Imran *et al.,* 2022). The rapid urbanization aimed at boosting economic conditions has impacted the local ecology to varying extents, rendering it more vulnerable to land degradation (Hasan *et al.,* 2020). There is a significant expansion in urban areas as more individuals move to metropolitan regions in search of employment (Chakma *et al.,* 2023; Roy *et al.,* 2020). Several studies have explored the correlation between LUTs and Summer LST in Chattogram City (Miah *et al.,* 2023). Some studies have focused on exploring several heat indices to understand the impact of LUTs on LST in the study area (Kafy

et al., 2020; Roy *et al.,* 2020) and predicted the LULC and seasonal LST for Chattogram in 2029 and 2039. Furthermore, the heat-vulnerable areas in CMA have also been mapped in recent years (Raja *et al.,* 2021).

However, comprehensive ecological assessments of CMA to understand its transformations and the impact of LUTs on ecological quality are lacking, both on small and large scales. Additionally, the existing literature does not provide a clear explanation for the relationship between the numerous indices examined. This study focuses on the spatiotemporal changes in EEQ in the CMA with three distinct aims. In the beginning, we used four specific indices, specifically NDVI, LST, NDBSI, and WET, to conduct a comprehensive spatiotemporal assessment of ecological quality within the CMA. Then we delved into the exploration of the impact of land use practices on the area's ecological health. Finally, we examined the interrelationships between these indices to understand their combined effectiveness in assessing ecological quality. This paper is innovative for two main reasons. Firstly, while most previous assessments in Bangladesh relied on unreliable surveys, our study used the RSEI with Landsat imagery data to evaluate environmental conditions and changing patterns. Secondly, we leveraged the powerful cloud computing capabilities of GEE to establish a consistent time threshold for the periods studied. Additionally, we enhanced the quality of the original images using cloud removal and image median equalization techniques. This comprehensive study is the first of its kind in CMA as well as in Bangladesh which will aid policymakers in formulating strategies for ecological and environmental conservation to the greatest extent.

2. Materials and Methods

2.1 Study Area

The CMA is situated in the southeastern part of Bangladesh (Fig 1). This area lies between approximately 22°06' and 22°34' north latitude and 91°40' and 92°2' east longitude, covering approximately 720 km^2. CMA is geographically bordered by the Halda River and the Karnafuli River to the northeast and southwest, respectively, while the Rangamati district to the east and the Bay of Bengal to the west (Rahman *et al.,* 2017). The region experiences an annual average temperature varying from 13.5 °C to 32.5 °C, with a mean annual rainfall of 3378 mm (Ahmed *et al.,* 2018). CMA is characterized by a varied terrain, ranging from coastal plains to hilly tracts, influencing local climatic patterns and land use dynamics. The landscape features a mix of natural ecosystems, including coastal belts, low-lying wetlands, and hills covered with

vegetation. Urbanized zones comprise a significant portion of the area, with densely populated neighborhoods, industrial estates, and commercial hubs.

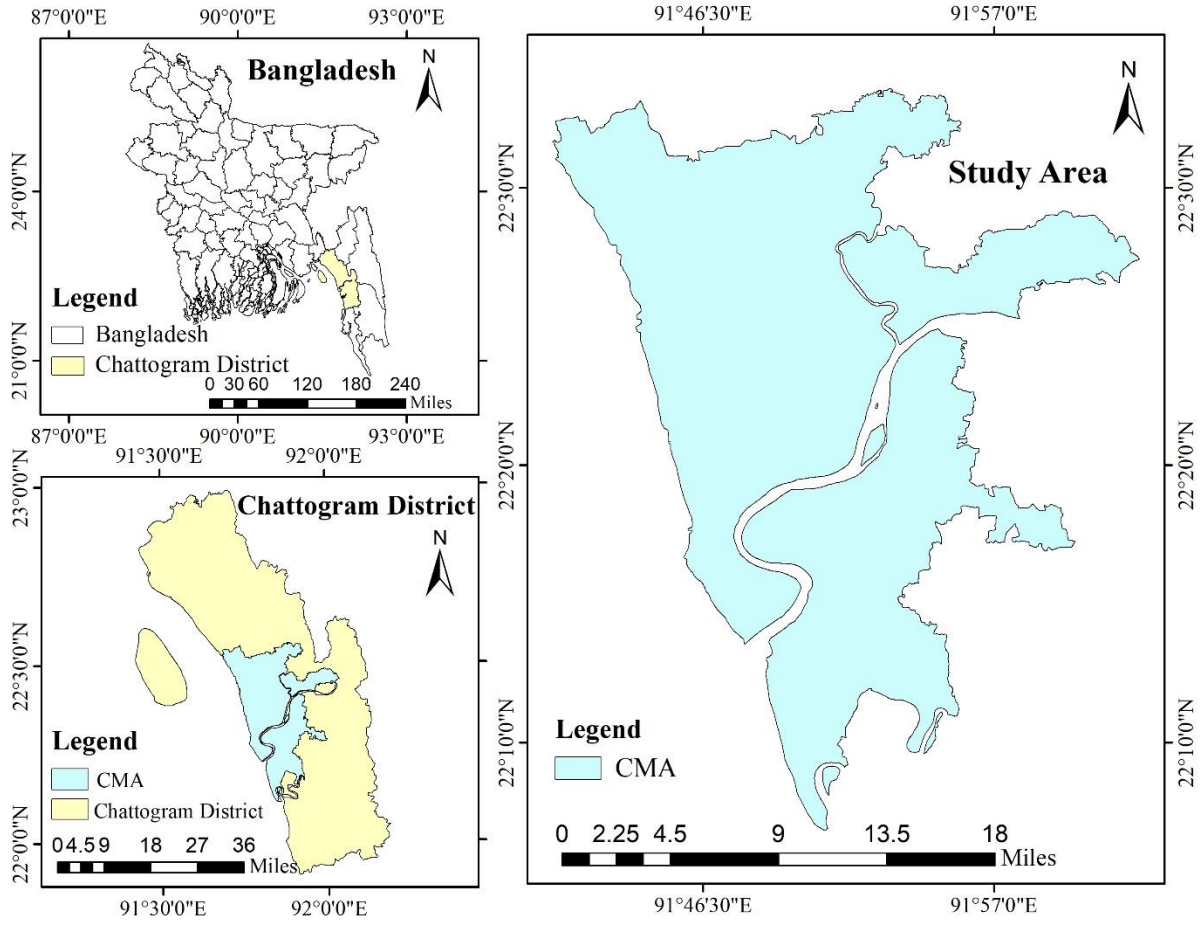

Fig. 1 Chattogram metropolitan area in Bangladesh.

2.2 Data source

This paper investigates the characteristics of the spatio-temporal variation of the EEQ in CMA in 2003, 2013, and 2023. Fig 2 presents a comprehensive outline of the study's workflow. To achieve this, an RSEI model was developed using principal component analysis (PCA) and Landsat satellite images from the GEE (https://earthengine.google.org/) platform as the data source. RSEI was constructed as a dependent variable using the four indices: NDVI, LST, WET, and NDBSI as independent variables. We used Landsat imagery during the best growth season (March–April) every year to reduce the uncertainty driven by seasonal variations. Additionally, a quality control band is employed to remove cloud shadows from satellite images. The water influence was eliminated from each indication by masking the water with the normalized difference water index (NDWI). To ensure reliability, all raster images were reprojected to the WGS_1984_UTM_Zone_46N for further analysis.

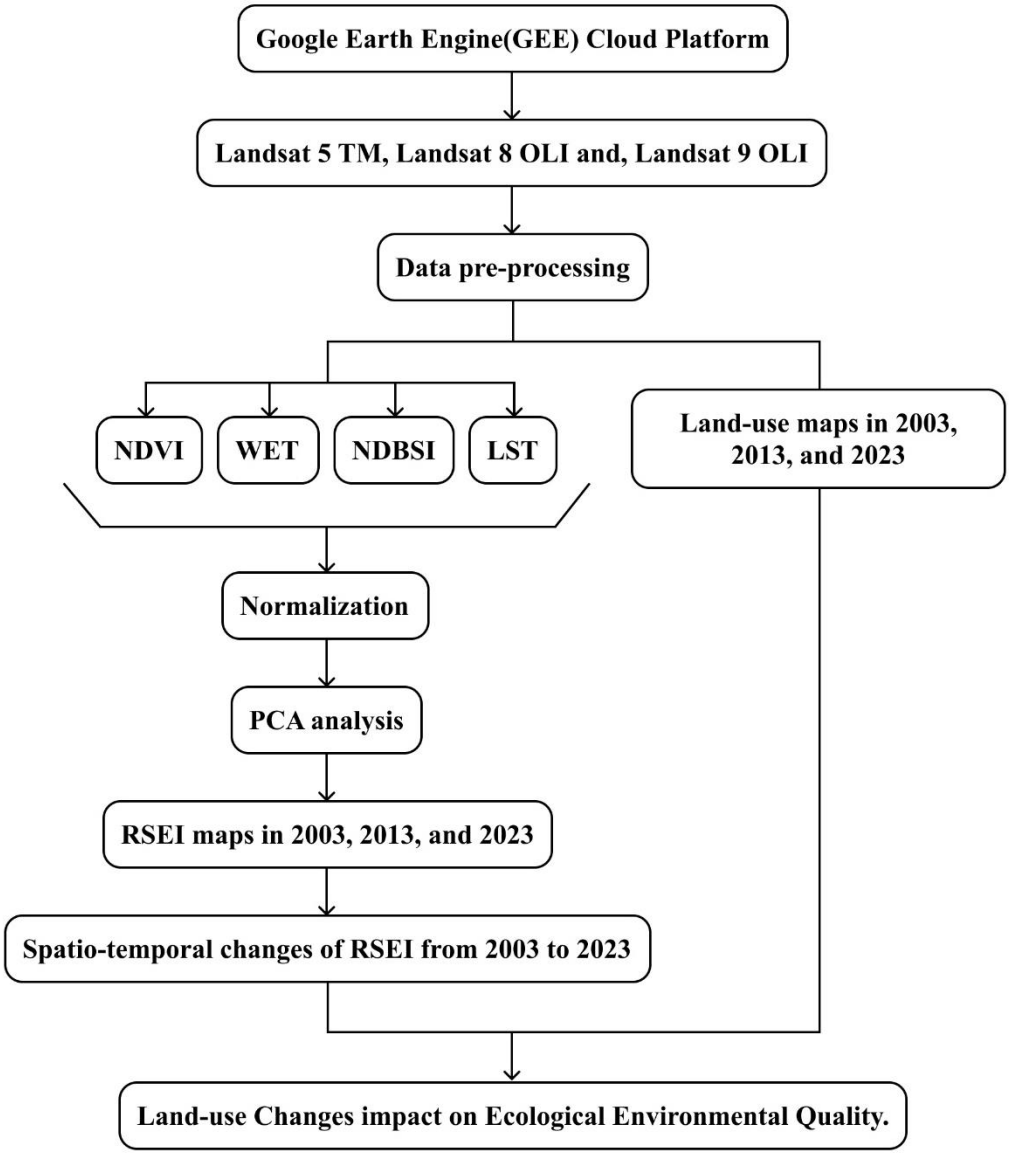

Fig. 2 Flow diagram of the methodology used for this study.

2.3 Land use land cover classification

Land-use maps of the study area were obtained using supervised classifications performed on Landsat TM+OLI imageries in 2003, 2013, and 2023. The random forest algorithm in the GEE platform was used for this purpose. The land use is categorized into five classes: vegetation, cropland, water body, urban areas, and bare land. To assess the accuracy of the classification process, a confusion matrix was used to calculate the Kappa index, as well as the overall user's and producer's accuracy (Congalton 1991). The overall classification accuracy of each LULC map ranged from 0.76% to 0.81% (Table 2).

2.4 Remote sensing-based ecological index

Relying solely on remote-sensing data, RSEI serves as a comprehensive tool for swift assessment of ecological and environmental conditions in any specific geographic area. There, we calculate the RSEI index by integrating four indices: NDVI, WET, LST, and NDBSI. ArcGIS 10.8 software normalizes each index [0, 1] after calculating these indices in GEE. This software then performs PCA, and the output PC1 (first principal component) represents the initial value of RSEI. Finally, we generated the normalized RSEI by following Eq. (1) in the raster calculator.(Airiken *et al.,* 2022; Mao *et al.,* 2023; Su *et al.,* 2023; Wang *et al.,* 2022).

$$RSEI = \frac{(PC1 - PC1_{min})}{(PC1_{max} - PC1_{min})} \quad (1)$$

Where $PC1_{min}$ and $PC1_{max}$ represent the minimum and maximum value of PC1.

2.4.1 Normalized Difference Vegetation Index

NDVI emerged as the most popular vegetation index in remote sensing applications. This index is extensively employed to identify and quantify the presence of green vegetation on terrestrial surfaces. In the context of remote sensing ecological assessments, the degree of greenness is described by the following eq. (2) in the ecological index proposed by (Rouse *et al.,* 1973).

$$NDVI = \frac{(\rho NIR - \rho red)}{(\rho NIR + \rho red)} \quad (2)$$

Here, ρNIR and ρRed are represented as the near-infrared band and red bands.

2.4.2 Wetness

Tassel cap transformation facilitates the extraction of moisture, which is then expressed through the resulting wet component (Zhang *et al.,* 2022). However, one needs to understand that the coefficients associated with these components exhibit variability depending on the sensor used. The calculation of the wet component in Landsat 5 and Landsat 8 can be performed according to the following eq.(3) and eq.(4) (Lobser and Cohen 2007; Wang *et al.,* 2023).

Landsat 5 TM,

$$Wet = 0.3102\rho Red + 0.1594\rho NIR + 0.0315\rho Blue + 0.2021\rho Green - 0.6806\rho SWIR1 - 0.6109\rho SWIR2 \quad (3)$$

Landsat 8 OLI/TIRS,

$$Wet = 0.3283\rho Red + 0.3407\rho NIR + 0.1511\rho Blue + 0.1973\rho Green - 0.7171\rho SWIR1 - 0.4559\rho SWIR2 \quad (4)$$

$\rho Red, \rho Green$, and $\rho Blue$ represent as red, green, and blue bands. $\rho SWIR$ and ρNIR represent as shortwave and near-infrared bands.

2.4.3 Land surface temperature

The single-chain method was used to estimate LST for this study area (Jimenez-Munoz *et al.,* 2009, 2014; Roy and Bari 2022; Sobrino *et al.,* 2004). The following equations were utilized to calculate LST in GEE platform.

$$LST = \frac{T_b}{1 + \left(\lambda * \frac{T_b}{\rho}\right) ln\varepsilon} \quad (5)$$

T_b represents the brightness temperature calculated by following the formula,

$$T_b = \frac{k_2}{\ln\left(k_1/L_\lambda + 1\right)} \quad (6)$$

$$L_\lambda = Gain * DN + Bias \quad (7)$$

L_λ represent the amount of electromagnetic energy emitted from a surface. Gain and Bias are calibration coefficients that are specific to each Landsat band. They are applied to the DN value to account for variations in sensor response and to convert the DN to a physical unit of radiance.

k_1 and k_2 are the thermal conversion constant for Landsat 5 TM and Landsat 8 OLI. For the TM sensor, k_1 and k_2 respectively 607.76 mW cm^{-2} and 1260.56 K. for the OLI sensor, $k_1$and k_2 respectively 774.89 mW cm^{-2} and 1321.08 K (Karbalaei Saleh *et al.,* 2021; Yue *et al.,* 2019). λ indicates the wavelength for thermal band (11.435 μm for Landsat 5 TM and 10.9 μm for Landsat 8 OLI), ρ is the constant value (1.438×10^{-2} mK), and ε denotes the emissivity which is calculated as follows:

$$Emissivity\ (\varepsilon) = 0.004 * pv + 0.986 \quad (8)$$

Where, pv represent the proportion of vegetation. Minimum and maximum value of $NDVI$ and following eq.(9) used to calculate the pv

$$Proportion\ of\ vegetation\ (pv) = \left[\frac{(NDVI - NDVI_{min})}{(NDVI_{max} - NDVI_{min})}\right]^2 \quad (9)$$

2.4.4 Normalized difference built-up soil index

NDBSI recognized for its efficacy in assessing dryness, involves the averaging of two indices: The built-up index (IBI) and the soil index (SI) (Liu *et al.,* 2022). These indices characterize

the respective conditions of urban areas and bare land (Hu and Xu 2018). NDBSI is calculated as follows:

$$IBI = \frac{\{2\rho SWIR1 / (\rho SWIR1 + \rho NIR) - [\rho NIR / (\rho NIR + \rho Red) + \rho Green / (\rho Green + \rho SWIR1)]\}}{\{2\rho SWIR1 / (\rho SWIR1 + \rho NIR) + [\rho NIR / (\rho NIR + \rho Red) + \rho Green / (\rho Green + \rho SWIR1)]\}} \quad (10)$$

$$SI = \frac{[(\rho SWIR1 + \rho Red) - (\rho Blue + \rho NIR)]}{[(\rho SWIR1 + \rho Red) + (\rho Blue + \rho NIR)]} \quad (11)$$

$$NDBSI = \frac{(\mathrm{IBI} + \mathrm{SI})}{2} \quad (12)$$

In order to uniform these four indices, should be normalized [0,1]. The normalization process is as follows:

$$Normalized\ Index = \frac{Index - Index_{min}}{Index_{max} - Index_{min}} \quad (13)$$

Here, $Index_{min}$ and $Index_{max}$ define the minimum and maximum value of the index, respectively.

2.5 Principal Component Analysis

PCA is a statistical technique that is used for data reduction, identifying the components that are responsible for the overall variability within the values taken into account (Akbar *et al.,* 2022; Li *et al.,* 2021). Additionally, it is used in the scientific arena for various purposes e.g. extracting and identifying the initial components, selecting the significant elements that are to be retained in the model (Petrişor *et al.,* 2012). In this study, four specific ecological factors named NDVI, LST, NDBSI, and WET are used, and then calculate the RSEI through PCA using ArcGIS 10.8 software.

3. Results

3.1 Spatial-temporal changes of LULC

The use and arrangement of land significantly impacts ecosystem health and overall environmental well-being, serving as vital determinants of habitat quality, biodiversity, and resource availability (Yang *et al.,* 2019). Over the past two decades, from 2003 to 2023, we classified the CMA into five distinct LULC classes. These classes include vegetation, cropland, water bodies, urban areas, and bare land. Vegetation primarily occupied the hilly terrains located in the northwest and southern regions of the study area, forming dense patches that serve as crucial biodiversity hotspots and contribute to ecological stability by providing

essential ecosystem services, such as carbon sequestration and soil erosion prevention. The study region predominantly found crops in areas adjacent to major rivers, distributing them sporadically to capitalize on fertile soils and water access for agricultural productivity. This extensive cropland supports the regional economy, providing food security and employment opportunities for local communities. Meanwhile, economic activities, population growth, and infrastructure development have driven rapid urbanization trends, resulting in a dense concentration of urban land in the central part of the CMA. This transformation into built-up areas has implications for both environmental health, particularly through increased pollution and the urban heat island effect, as well as social dynamics, such as housing demand and congestion. We observed scattered water ponds, including lakes, reservoirs, and small ponds, throughout the region, providing critical ecosystem services such as freshwater supply, climate regulation, and aquatic habitats. However, these water bodies often appeared fragmented, likely indicating anthropogenic pressures such as encroachment or over-extraction (Fig 3). Lastly, areas unsuitable for either agriculture or urban expansion primarily featured bare land, mostly composed of exposed soil and rocky outcrops. These areas, while naturally occurring in some cases, could also represent degraded land, potentially due to unsustainable agricultural practices, deforestation, or construction activities. The dynamic interplay among these LULC classes over time provides insight into the shifting landscape patterns of the CMA and highlights the need for sustainable land management practices to ensure balanced environmental health.

Table 1 LULC area in CMA from 2003 to 2023.

LULC Types	**Years**					
	2003		**2010**		**2023**	
	Area (km^2)	Area (%)	Area (km^2)	Area (%)	Area (km^2)	Area (%)
Vegetation	334.97	46.25	318.95	44.04	258.06	35.63
Cropland	313.64	43.3	288.19	39.79	307.89	42.51
Waterbody	18.65	2.58	13.96	1.93	15.76	2.18
Urban	34.08	4.71	80.38	11.1	101.98	14.08
Bare Land	22.91	3.16	22.77	3.14	40.56	5.6

Table 2 Accuracy assessment of LULC maps.

LULC Types	**Years**					
	2003		**2013**		**2023**	
	P	U	P	U	P	U
Vegetation	0.91	0.79	0.89	0.84	1.00	1.00
Cropland	0.94	0.84	0.74	0.82	0.91	0.78
Waterbody	0.94	1.00	0.93	1.00	1.00	0.89
Urban	0.76	0.78	0.89	0.75	0.69	0.79
Bare Land	0.70	0.74	0.50	0.74	0.72	0.67

Overall accuracy (%)	0.81	-	0.78	-	0.76	-
Kappa coefficient	0.75	-	0.67	-	0.66	-

257 * p: producer accuracy; U: user accuracy

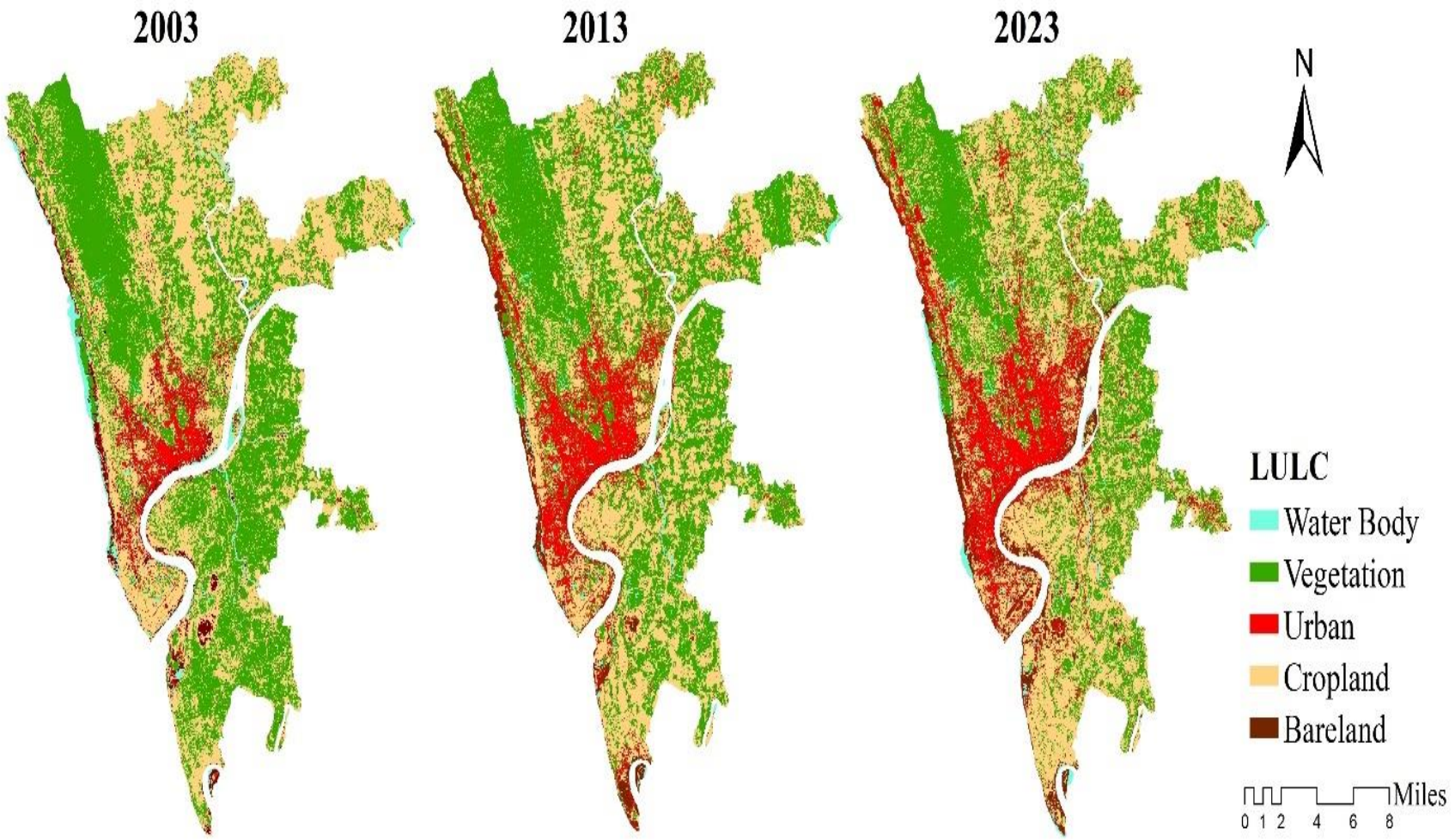

Fig 3: Spatial distribution of LULC in CMA from 2003 to 2023.

Table 1 shows that more than 77% of the land was covered by vegetation and cropland, indicating the strong presence of forestry and agriculture in the area. The coverage of vegetation and cropland decreased significantly from 46.25% (334.98 km^2) and 43.31% (313.64 km^2) in 2003 to 35.63% (258.06 km^2) and 42.51% (307.89 km^2) in 2023, respectively. The LULC classes showed a gradual expansion in urban areas over the last two decades, indicating social progress. The urban area expanded from 34.08 km^2 (4.71%) in 2003 to 101.99 km^2 (14.08%) in 2023, an increase of 67.91 km^2 in 20 years. The annual expansion rate was 2.34 km^2 (0.46%) % each year. This growth is linked to the city's GDP which increased from $16 billion in 2005 to $39 billion in 2020 (Miah and Hossain 2022). All classes, excluding urban areas and bare land, experienced a decrease, with the vegetation class showing the largest decline.

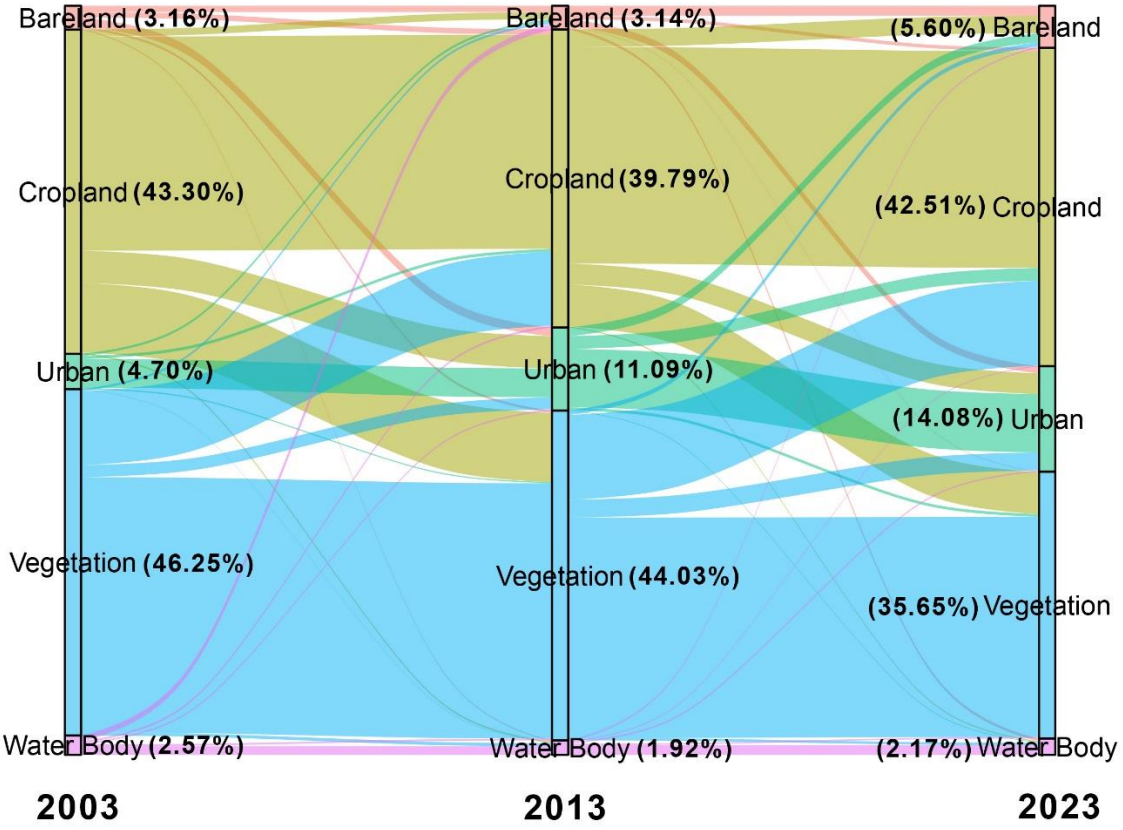

Fig. 4 LULC transition from 2003 to 2023 using Sankey Diagram.

The LULC transfer matrix was used to create a Sankey diagram (Fig 4) that effectively illustrates the origin and destination of each land use category qualitatively and quantitatively. From the Fig

4, it shows that vegetation land holds a dominant position and tends to decline. Moreover, the vegetation land is not only transferred within its category but primarily transferred to cropland and urban land. During 2013-2023, most of the vegetated land was converted to cropland and urban land, covering 81.99 km² and 17.34 km² respectively. Cropland follows as the second most converted land type, with a significant portion being transferred to vegetation and urban land at 67.13 km^2 and 31.174 $km^{2,}$ respectively, from 2003 to 2013. Conversely, urban and bare land, along with water bodies, exhibit comparatively lower transfer volumes. From 2003 to 2023, urban areas in CMA increased the most among all types of land use. In CMA, urban lands are mostly composed of converted cropland, vegetation, and bare land. This rapid urbanization is leading to ecological degradation and impacting SDGs in the region.

3.2 Spatial-temporal changes in ecological quality

The research analyzed various ecological factors like NDVI, LST, NDBSI, and WET to calculate the RSEI through PCA using ArcGIS 10.8 software. The PCA results of CMA in 2003, 2013, and 2023 are tabulated. According to Table 3**,** PC1 eigenvalues had a contribution rate of over 80%. This indicates that the first principal component accurately represents the important features of each factor. The NDVI and WET index from 2003 to 2023 are positive values, indicative of their constructive impact on the local ecological landscape. On the contrary, the NDBSI and LST showed adverse values, suggesting a detrimental influence impeding ecological restoration and enhancement efforts within the study area.

Table 3: PCA dataset of RSEI.

Year	Indices	PC1	PC2	PC3	PC4	Mean RSEI
2003	NDVI	0.676	-0.543	0.428	0.254	0.616
	LST	-0.311	0.327	0.892	0.022	
	NDBSI	-0.628	-0.550	-0.031	0.549	
	WET	0.227	0.543	-0.140	0.796	
	Eigenvalue	0.018	0.002	0.001	0.000	
	Percentage	84.91	8.07	6.67	0.35	
2013	NDVI	0.711	-0.010	0.696	0.098	0.627
	LST	-0.353	0.859	0.370	0.015	
	NDBSI	-0.599	-0.495	0.566	0.275	
	WET	0.105	0.130	-0.239	0.956	
	Eigenvalue	0.019	0.001	0.001	0.000	
	Percentage	88.98	6.57	4.37	0.08	
2023	NDVI	0.720	-0.027	0.666	0.194	0.621
	LST	-0.326	0.866	0.377	0.035	
	NDBSI	-0.576	-0.435	0.453	0.524	
	WET	0.209	0.245	-0.458	0.829	
	Eigenvalue	0.017	0.002	0.001	0.000	
	Percentage	82.83	10.40	6.53	0.25	

To better understand the ecological environment's changes and attributes within the study area, the RSEI has been categorized into five distinct levels based on pertinent literature: worst (0–0.2), poor (0.2–0.4), moderate (0.4–0.6), good (0.6–0.8), and excellent (0.8–1) (Su *et al.,* 2023; Sun *et al.,* 2022; X. Wang *et al.,* 2022). Over the period of 2003 to 2023, the average RSEI in the study area was above 0.6. This indicates that all areas in the study were rated as good according to the RSEI classification criteria.

The temporal and spatial distribution of the EEQ of the study area has been shown in Fig 5 from 2003 to 2023. In 2003, there were small and scattered areas with low EEQ, particularly clustered near Bangladesh's main seaport. Human activities significantly affected these areas, which were mostly on the outskirts of the main urban area. The hilly regions in the northeast and south exhibited excellent EEQ. The agricultural lands primarily range from good to moderate EEQ levels. The red areas with poor EEQ gradually expanded over the next few years, particularly in 2008, 2014, and 2018, demonstrating a polycentric clustering expansion trend compared to the baseline in 2003.

Table 4 RSEI area calculation.

Grade/years	Worst (0-0.2)		Poor (0.2-0.4)		Moderate (0.4-0.6)		Good (0.6-0.8)		Excellent (0.8-1)	
	Area (km^2)	%	Area (km^2)	%	Area (km^2)	%	Area (km^2)	%	Area (km^2)	%
2003	4	0.6	68	10.0	213	31.2	316	46.3	81	11.9
2013	9	1.3	72	10.6	175	25.7	321	47.1	104	15.3
2023	5	0.7	71	10.4	181	26.6	362	53.2	62	9.1

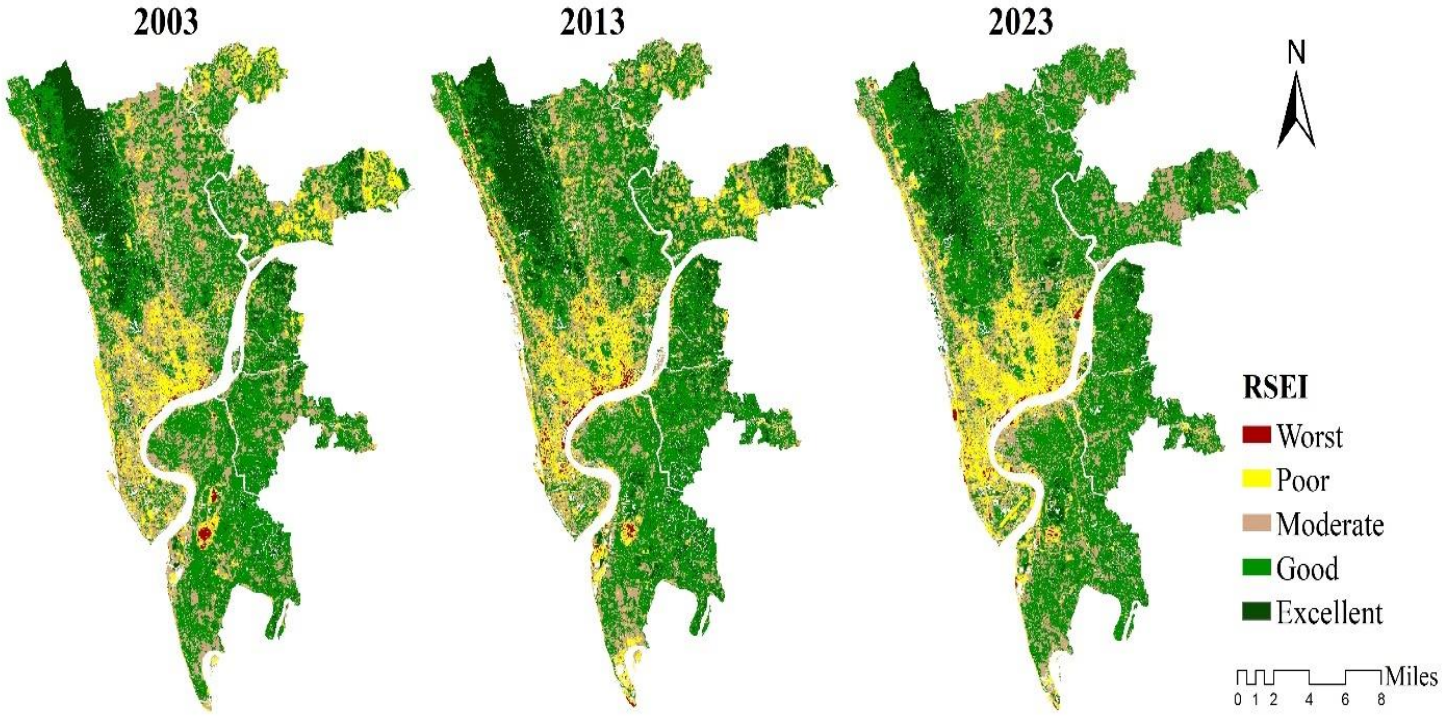

Fig. 5 Spatial distribution of RSEI in CMA from 2003 to 2023.

The study examined the size and proportion of each ecological grade within the study area over three different years (Table 4). In 2003, the study area was 681 km², with 71 km² classified as worst EEQ and 71 km² as poor EEQ, making up 10.4% of the total area. By 2013, this percentage increased but then decreased to 11.1% by 2023. Moderate EEQ land was 213 km² in 2003, accounting for 31.3% of the total area. This decreased to 25.7% by 2013 and slightly increased to 26% by 2023. Land with good EEQ levels showed a gradual increase from 2003 to 2023. Excellent EEQ areas were 11.9% in 2003, increased to 15.3% by 2013, but decreased to 9.1% by 2023, indicating a conversion of vegetation land to cropland or urban areas.

The changes in RSEI detection in CMA from 2003 to 2023 are illustrated in Fig 6. The ecological environment degradation was primarily focused on the central regions due to increased human activities. Urban construction and land-reclamation activities in the central and economic zones between 2003 and 2013 damaged the natural landscape and produced pollutants, affecting ecological quality.

Table 5 Dynamic change of ecological quality over the years.

Year	Improved (km^2)	%	Unchanged (km^2)	%	Degraded (km^2)	%
2003 – 2013	139	21.4	413	63.4	99	15.2
2013 – 2023	108	16.5	407	62.5	137	21.0
2003 – 2023	151	23.1	355	54.5	146	22.4

Between 2013 and 2023, urban construction on the island shifted to developing within the existing urban area because of the limited availability of appropriate land resources. This change resulted in a moderate decline in ecological quality. From 2003 to 2013, 63.4% of the entire area remained unchanged in ecological quality, accounting for 413 km^2 (Table 5). During this period, degenerated areas accounted for 15.2% of the entire area at 99 km^2, while improved regions covered 21.4% of the total area, which is 139 km. From 2013 to 2023, degraded areas accounted for 21% of the entire area, improved regions covered 16.5%, and unchanged areas comprised 62.5%. These findings indicate that the study area experienced more ecological degradation than improvement during this period. Comparing the entire span from 2003 to 2023, degraded areas constituted 22.4%, ecologically improved areas comprised 23.1%, and unchanged areas accounted for 54.5% of the

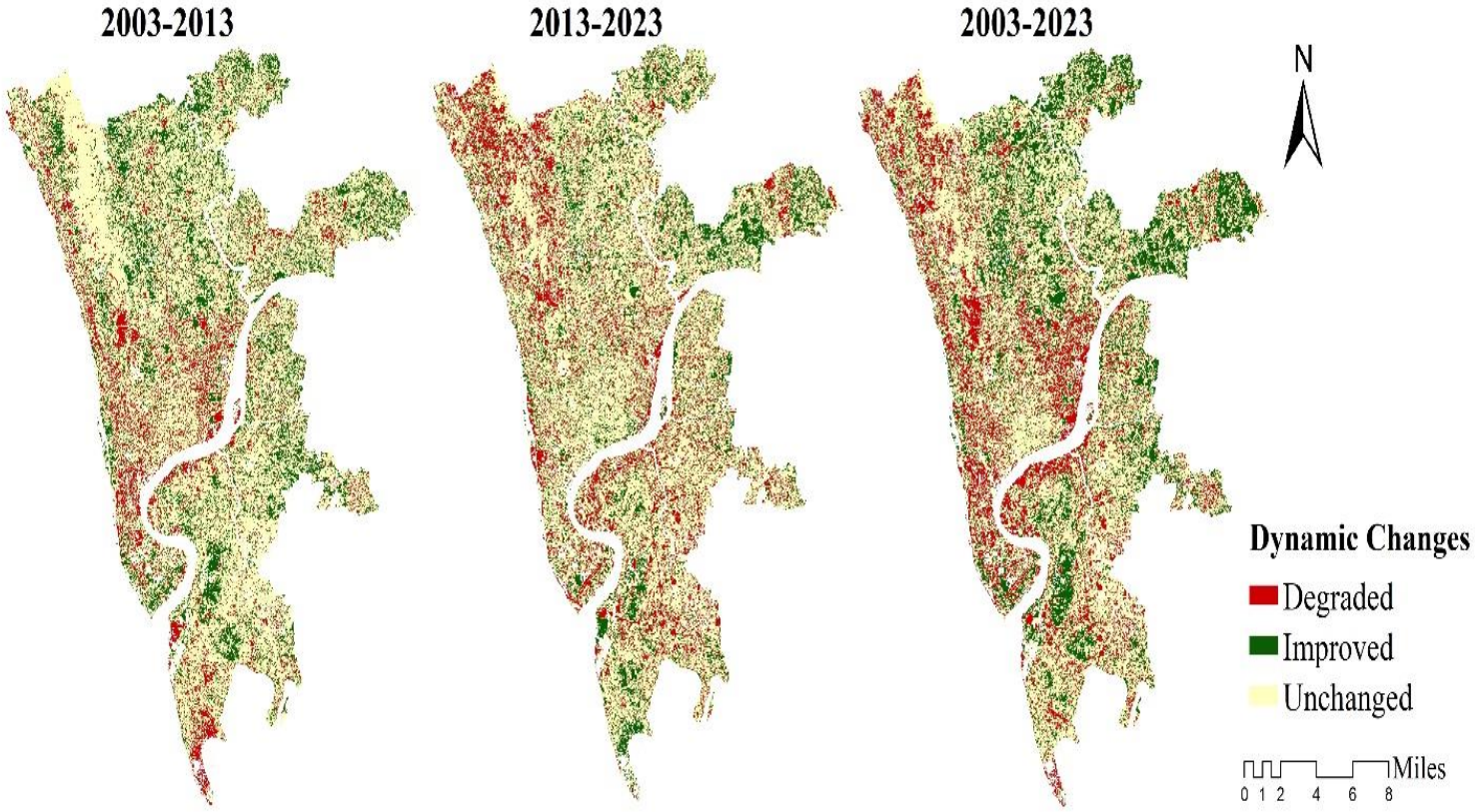

Fig. 6 Spatial changes in RSEI over 2003 to 2023.

study area. From 2003 to 2023, there were significant land transformations from forests and croplands to urban areas. However, the overall ecological quality did not see a significant decline during this period.

3.3 Land use responses to ecological quality

The images of Landsat 5 in 2003 and Landsat 8 in 2013 and 2023 were used in our experiment. They were also used to calculate the indices required to obtain the formulated RSEI and map land use. The RSEI was greatly impacted using scientific urban planning and ecological environment planning. We analyzed and processed data on land use type formation and the remote sensing ecological index to better understand the relationship between land use type and the ecological environment. As a result, we obtained the RSEI of each land use type (Fig 7). The study found differences in EEQ among different land use types. Compared to other land use types, vegetated land had the most RSEI value between 2003 and 2023. Furthermore, the RSEI values on bare and urban land were among the lowest.

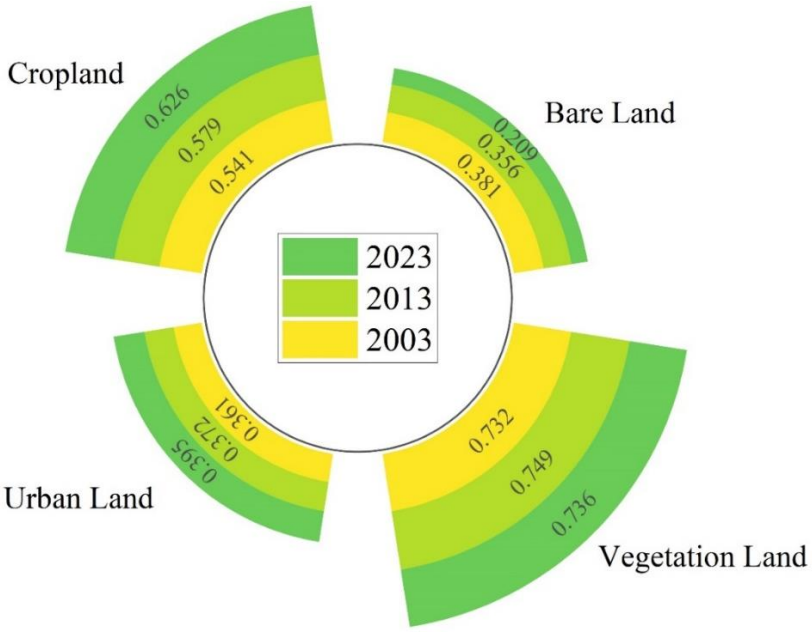

Fig. 7 RSEI value of each land use type from 2003 to 2023.

3.3 Correlation analysis among indices

For correlation analysis, the values of RSEI, NDVI, NDBSI, WET, and LST were extracted from the tabular format of the converted raster-to-point data of each image, using the 2013 Landsat image data as an example. We used Origin Pro to conduct correlation analysis. The results of the analysis can be seen in Fig 8. Green shading represents a positive correlation, with darker shades indicating a stronger positive correlation, while white indicates a negative correlation. The NDVI and WET indicators demonstrated a strong positive correlation (R^2 = 0.98, 0.83) with RSEI, whereas they exhibited a significant negative correlation (R^2 = -0.82, -0.96) with LST and NDBSI. A significant positive correlation (R^2 = 0.72) was observed between WET and NDVI, while a significant negative correlation (R^2 = -0.76, -0.89) was found with LST and NDBSI. WET and NDBSI displayed significant negative and positive correlations (R^2 = -0.61, 0.70) with LST, respectively. On the other hand, NDBSI exhibited a significant negative correlation (R^2 = -0.94) with WET. As a result, the research above suggests that there is a significant relationship between RSEI and each measure. RSEI is more reflective of overall ecological quality and more effectively synthesizes information from each variable when compared to the usage of individual remote sensing-based metrics. Therefore, the RSEI was utilized to represent the studied area's entire ecological quality.

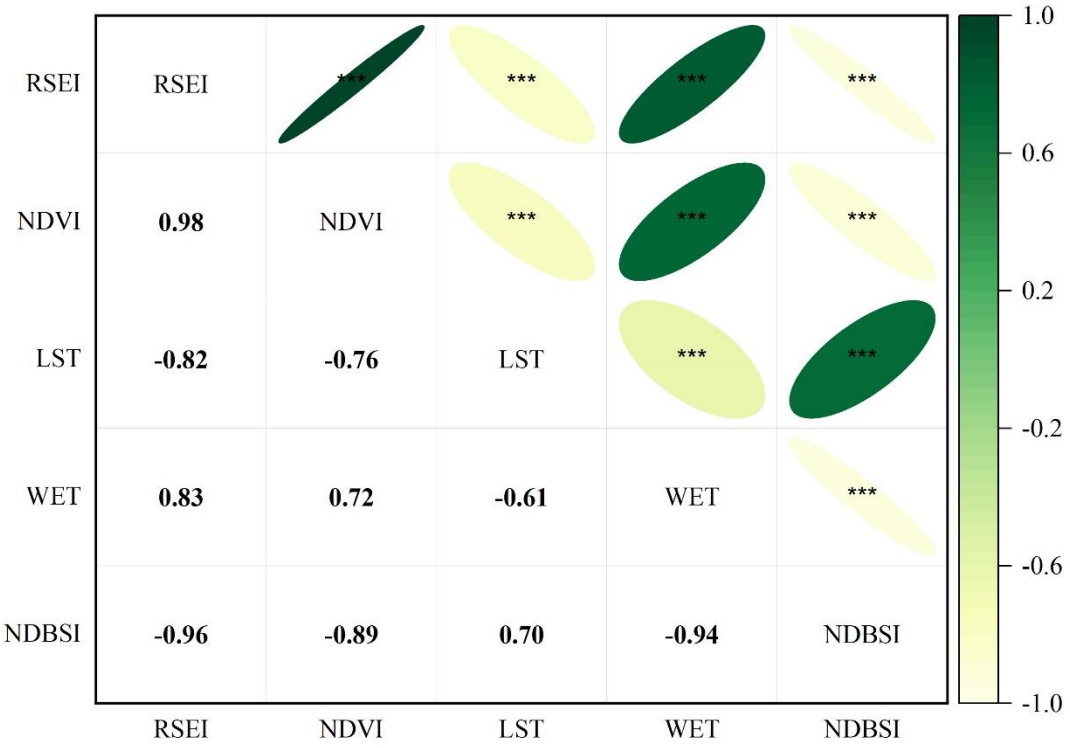

* p<=0.05 ** p<=0.01 *** p<=0.001

Fig. 8 Correlation matrix of RSEI.

4. Discussion

The GEE platform was employed to utilize the cloud-free images, and median equalization techniques were applied to enhance the original image quality. The platform allows for convenient access to extensive data at any time (Kumar and Mutanga 2018; Shelestov *et al.,* 2017; Wang *et al.,* 2022). The application of the Random Forest algorithm for land use classification demonstrated robust performance and high accuracy in distinguishing between different land cover types. During training, Random Forest creates several decision trees as a method of collaborative learning and outputs the mode of classes for each tree. This method successfully reduces the overfitting issue that distinct decision trees can have, improving the model's predictability (Gislason *et al.,* 2006; Svoboda *et al.,* 2022; Tikuye *et al.,* 2023). In this study, the Random Forest algorithm was particularly adept at handling the complexity and heterogeneity inherent in land use data. Unfortunately, to eradicate the detrimental effect of enormously water regions on the normalization process and eigenvalue of WET and NDBSI in the RSEI calculation, the NDWI was utilized in

this work to mask the large water areas (Acharya *et al.,* 2018). In other words, our research concentrated on assessing ecological quality in land regions rather than water bodies. PC1 eigenvalues had a contribution rate of over 80%. This indicates that the first principal component accurately represents the important features of each factor, which were like previous studies (Maity *et al.,* 2022; Wang *et al.,* 2022; Xu *et al.,* 2019). Our study showed that RSEI negatively correlated with LST and NDBSI, suggesting detrimental impacts, while NDVI and WET showed positive correlations, indicating beneficial effects. These findings are consistent with previous studies (Airiken *et al.,* 2022; Karbalaei Saleh *et al.,* 2021; Maity *et al.,* 2022; Mao *et al.,* 2023; Su *et al.,* 2023; Wang *et al.,* 2022; Xu *et al.,* 2019). The impact of the vegetation indication outweighed the other indicators (Table 2). The CMA's ecological quality ranged from 0.616 to 0.621, which is considered good quality. Ecological quality remained mostly stable and even showed a slight improvement. The RSEI was greatly impacted of scientific urban planning and ecological environment planning.

The RSEI values differed in various landscapes, such as 0.21-0.38 in barren areas and 0.36-0.39 in urban areas (Guo *et al.,* 2017; Yue *et al.,* 2019), greater than 0.73 in vegetation regions (Xu *et al.,* 2019), and even 0.54-0.63 in cropland (Shan *et al.,* 2019). The result of the RSEI value of each land use type supports that forests generally enhance the ecological quality of the land by supporting biodiversity, regulating climate and water cycles, and providing various ecosystem services. In contrast, construction land often degrades ecological quality through habitat destruction, soil degradation, increased stormwater runoff, heat island effects, and loss of green space. Sustainable land use planning and development practices are essential to mitigate the negative impacts of construction activities and preserve the ecological integrity of landscapes. There are two possible ways to apply the RSEI to SDG 15. I) RSEI is represented as an indicator for the construction industry which can be applied to make buildings more sustainable and affect the protection of wildlife and the environment. II) The RSEI is also used as an indicator for terrestrial ecosystems, and it has the potential to substitute the improved vegetation index and water network density that are included in the biological diversity indicator system to meet sustainable development goals.

5. Conclusion

This study examined the patterns of land use changes and their effects on the ecological quality of CMA over the two decades (2003-2023), which provide valuable insights for the sustainable development of the region's society, economy, and ecology. The key findings are as follows:

I. The study found significant decreases in vegetation and cropland, alongside substantial increases in urban areas over the past two decades, indicating social progress but potential negative impacts on ecological health due to urban expansion. The urban areas expanded annually at a rate of 2.34 km². The Sankey diagram showed that most new urban lands originated from cropland, vegetation, and bare land, with vegetation land largely being converted to cropland and urban land.

II. The NDVI and WET indices showed positive values from 2003 to 2023, indicating a positive impact on the local ecological landscape, while NDBSI and LST showed negative values, indicating a negative impact. Vegetation land had the highest RSEI values during this period, suggesting better ecological quality, whereas bare and urban land had the lowest RSEI values, suggesting worse ecological quality. Land with vegetation led to ecological improvement, while land converted to urban land led to ecological degradation.

III. All the indicators exhibited a significant linear correlation with RSEI and with each other. Furthermore, NDVI and NDBSI showed higher correlation coefficients than LST and WET.

This study helps policymakers understand the trade-offs and synergism among different development objectives. It highlights potential conflicts between economic growth and environmental sustainability, allowing policymakers to devise strategies that balance competing interests and maximize sustainable outcomes.

Statements & Declarations

Acknowledgements

The authors would like to acknowledge the anonymous reviewers and editors.

Declaration of competing interests

The authors declare no conflicts of interest.

Funding

This research received no specific grant from funding agencies in the public, commercial or not-for-profit sectors.

Data Availability

Data will be made available on request.

References

Acharya TD, Subedi A, and Lee DH (2018) Evaluation of water indices for surface water extraction in a landsat 8 scene of Nepal. Sensors, 18(8), 1–15. https://doi.org/10.3390/s18082580

Ahmed B, Rahman MS, Islam R, Sammonds P, Zhou C, Uddin K, Al-Hussaini TM (2018) Developing a dynamic web-GIS based landslide early warning system for the Chattogram metropolitan area, Bangladesh. ISPRS International Journal of Geo-Information, 7(12). https://doi.org/10.3390/ijgi7120485

Airiken M, Zhang F, Chan NW, Kung H (2022) Assessment of spatial and temporal ecological environment quality under land use change of urban agglomeration in the North Slope of Tianshan, China. Environmental Science and Pollution Research, 29(8):12282–12299. https://doi.org/10.1007/s11356-021-16579-3

Akbar TA, Javed A, Ullah S, Ullah W, Pervez A, Akbar RA, Javed MF, Mohamed A, and Mohamed AM (2022) Principal Component Analysis (PCA)–Geographic Information System (GIS) Modeling for Groundwater and Associated Health Risks in Abbottabad, Pakistan. Sustainability, 14(21). https://doi.org/10.3390/su142114572

Chakma M, Hayat U, Meng J, Hassan MA (2023) An Assessment of Landscape and Land Use/Cover Change and Its Implications for Sustainable Landscape Management in the Chattogram Hill Tracts, Bangladesh. Land, 12(8). https://doi.org/10.3390/land12081610

Congalton RG (1991) A review of assessing the accuracy of classifications of remotely sensed data. Remote Sensing of Environment, 37(1):35–46. https://doi.org/10.1016/0034-4257(91)90048-B

Costanza R, de Groot R, Sutton P, van der Ploeg S, Anderson SJ, Kubiszewski I, Farber S, Turner RK (2014) Changes in the global value of ecosystem services. Global Environmental Change, 26(1):152–158. https://doi.org/10.1016/j.gloenvcha.2014.04.002

Gislason, P. O. Benediktsson, J. A. and Sveinsson, J. R. (2006). Random forests for land cover classification. Pattern Recognition Letters, 27(4), 294–300. https://doi.org/10.1016/j.patrec.2005.08.011

Guo, H. Zhang, B. Bai, Y. and He, X. (2017). Ecological environment assessment based on Remote Sensing in Zhengzhou. IOP Conference Series: Earth and Environmental Science, 94(1). https://doi.org/10.1088/1755-1315/94/1/012190

Hariram NP, Mekha KB, Suganthan V, Sudhakar K (2023) Sustainalism: An Integrated Socio-Economic-Environmental Model to Address Sustainable Development and Sustainability. Sustainability, 15(13). https://doi.org/10.3390/su151310682

Hasan SS, Sarmin NS, Miah MG (2020) Assessment of scenario-based land use changes in the Chattogram Hill Tracts of Bangladesh. Environmental Development, 34. https://doi.org/10.1016/j.envdev.2019.100463

Hu X, Xu H (2018) A new remote sensing index for assessing the spatial heterogeneity in urban ecological quality: A case from Fuzhou City, China. Ecological Indicators, 89:11–21. https://doi.org/10.1016/j.ecolind.2018.02.006

Imran HM, Hossain A, Shammas MI, Das MK, Islam MR, Rahman K, Almazroui M (2022) Land surface temperature and human thermal comfort responses to land use dynamics in Chattogram city of Bangladesh. Geomatics, Natural Hazards and Risk, 13(1):2283–2312. https://doi.org/10.1080/19475705.2022.2114384

Ji J, Wang S, Zhou Y, Liu W, Wang L (2020) Spatiotemporal Change and Landscape Pattern Variation of Eco-Environmental Quality in Jing-Jin-Ji Urban Agglomeration from 2001 to 2015. IEEE Access, 8:125534–125548. https://doi.org/10.1109/ACCESS.2020.3007786

Jimenez-Munoz JC, Cristobal J, Sobrino JA, Sòria G, Ninyerola M, Pons X (2009) Revision of the single-channel algorithm for land surface temperature retrieval from landsat thermal-infrared data. IEEE Transactions on Geoscience and Remote Sensing, 47(1):339–349. https://doi.org/10.1109/TGRS.2008.2007125

506 Jimenez-Munoz JC, Sobrino JA, Skokovic D, Mattar C, Cristobal J (2014) Land surface
507 temperature retrieval methods from landsat-8 thermal infrared sensor data. IEEE
508 Geoscience and Remote Sensing Letters, 11(10):1840–1843.
509 https://doi.org/10.1109/LGRS.2014.2312032

510 Kafy A Al, Rahman MS, Faisal A Al, Hasan MM, Islam M (2020) Modelling future land use land
511 cover changes and their impacts on land surface temperatures in Rajshahi, Bangladesh.
512 Remote Sensing Applications: Society and Environment, 18.
513 https://doi.org/10.1016/j.rsase.2020.100314

514 Karbalaei Saleh S, Amoushahi S, Gholipour M (2021) Spatiotemporal ecological quality
515 assessment of metropolitan cities: a case study of central Iran. Environmental Monitoring and
516 Assessment, 193(5). https://doi.org/10.1007/s10661-021-09082-2

517 Kumar L, Mutanga O (2018) Google Earth Engine applications since inception: Usage, trends, and
518 potential. Remote Sensing, 10(10):1–15. https://doi.org/10.3390/rs10101509

519 Li J, Gong J, Guldmann JM, Yang J (2021) Assessment of urban ecological quality and spatial
520 heterogeneity based on remote sensing: A case study of the rapid urbanization of wuhan
521 city. Remote Sensing, 13(21). https://doi.org/10.3390/rs13214440

522 Li Y, Wu L, Han Q, Wang X, Zou T, and Fan C (2021). Estimation of remote sensing based
523 ecological index along the Grand Canal based on PCA-AHP-TOPSIS methodology.
524 Ecological Indicators, 122. https://doi.org/10.1016/j.ecolind.2020.107214

525 Liao W, Jiang W (2020) Evaluation of the spatiotemporal variations in the eco-environmental
526 quality in China based on the remote sensing ecological index. Remote Sensing, 12(15).
527 https://doi.org/10.3390/RS12152462

528 Liu Q, Yu F, Mu X (2022) Evaluation of the Ecological Environment Quality of the Kuye River
529 Source Basin Using the Remote Sensing Ecological Index. International Journal of
530 Environmental Research and Public Health, 19(19).
531 https://doi.org/10.3390/ijerph191912500

Lobser SE, Cohen WB (2007) MODIS tasselled cap: land cover characteristics expressed through transformed MODIS data. International Journal of Remote Sensing, 28(22):5079–5101. https://doi.org/10.1080/01431160701253303

Long H, Zhang Y, Ma L, Tu S (2021) Land use transitions: Progress, challenges and prospects. Land, 10(9). https://doi.org/10.3390/land10090903

Lu C, Shi L, Fu L, Liu S, Li J, Mo Z (2023) Urban Ecological Environment Quality Evaluation and Territorial Spatial Planning Response: Application to Changsha, Central China. International Journal of Environmental Research and Public Health, 20(4). https://doi.org/10.3390/ijerph20043753

Lu L, Weng Q, Guo H, Feng S, Li Q (2019) Assessment of urban environmental change using multi-source remote sensing time series (2000–2016): A comparative analysis in selected megacities in Eurasia. Science of the Total Environment, 684:567–577. https://doi.org/10.1016/j.scitotenv.2019.05.344

Ma X, Zhang H (2023) Land-Use/Land-Cover Change and Ecosystem Service Provision in Qinghai Province, China: From the Perspective of Five Ecological Function Zones. Land, 12(3). https://doi.org/10.3390/land12030656

Maity S, Das S, Pattanayak JM, Bera B, and Shit PK (2022). Assessment of ecological environment quality in Kolkata urban agglomeration, India. Urban Ecosystems, 25(4), 1137–1154. https://doi.org/10.1007/s11252-022-01220-z

Mao S, She J, Zhang Y (2023) Spatial-Temporal Evolution of Land Use Change and Eco-Environmental Effects in the Chang-Zhu-Tan Core Area. Sustainability, 15(9). https://doi.org/10.3390/su15097581

McCourt RM, Lewis LA, Strother PK, Delwiche CF, Wickett NJ, de Vries J, Bowman JL (2023) Green land: Multiple perspectives on green algal evolution and the earliest land plants. American Journal of Botany, 110(5). John Wiley and Sons Inc. https://doi.org/10.1002/ajb2.16175

Miah MD, Hasnat GNT, Nath B, Saeem MGU, Rahman MM (2023) Spatial and Temporal Changes in the Urban Green Spaces and Land Surface Temperature in the Chattogram City

Corporation of Bangladesh Between 2000 and 2020. Forestist 73(2):171–182. https://doi.org/10.5152/forestist.2022.22013

Miah MD, Hossain A (2022) Greenhouse Gas Emission Due to Plastic Waste Recycling in the Chattogram City Corporation. The Chattogram University Journal of Science 43(1):113–128. https://doi.org/10.3329/cujs.v43i1.57335

Petrişor AI, Ianoş I, Iurea D, and Văidianu MN (2012). Applications of Principal Component Analysis Integrated with GIS. Procedia Environmental Sciences, 14, 247–256. https://doi.org/10.1016/j.proenv.2012.03.024

Prăvălie R, Sîrodoev I, Nita IA, Patriche C, Dumitraşcu M, Roşca B, Tişcovschi A, Bandoc G, Săvulescu I, Mănoiu V, Birsan MV (2022) NDVI-based ecological dynamics of forest vegetation and its relationship to climate change in Romania during 1987–2018. Ecological Indicators 136:108629. https://doi.org/10.1016/j.ecolind.2022.108629

Rahaman MA, Kalam A, Al-Mamun M (2023) Unplanned urbanization and health risks of Dhaka City in Bangladesh: uncovering the associations between urban environment and public health. Frontiers in Public Health 11:1269362. https://doi.org/10.3389/fpubh.2023.1269362

Rahman MM, Huq H, Mukul SA (2023) Implications of Changing Urban Land Use on the Livelihoods of Local People in Northwestern Bangladesh. Sustainability 15(15):11769. https://doi.org/10.3390/su151511769

Rahman MS, Ahmed B, Di L (2017) Landslide initiation and runout susceptibility modeling in the context of hill cutting and rapid urbanization: a combined approach of weights of evidence and spatial multi-criteria. Journal of Mountain Science 14(10):1919–1937. https://doi.org/10.1007/s11629-016-4220-z

Raja DR, Hredoy MSN, Islam MK, Islam KMA, Adnan MSG (2021) Spatial distribution of heatwave vulnerability in a coastal city of Bangladesh. Environmental Challenges 4:100122. https://doi.org/10.1016/j.envc.2021.100122

Rouse J, Haas RH, Schell JA, Deering D (1973) Monitoring vegetation systems in the great plains with ERTS.

588 Roy B, Bari E (2022) Examining the relationship between land surface temperature and landscape
589 features using spectral indices with Google Earth Engine. Heliyon 8(9).
590 https://doi.org/10.1016/j.heliyon.2022.e10668

591 Roy S, Pandit S, Eva EA, Bagmar MSH, Papia M, Banik L, Dube T, Rahman F, Razi MA (2020)
592 Examining the nexus between land surface temperature and urban growth in Chattogram
593 Metropolitan Area of Bangladesh using long term Landsat series data. Urban Climate
594 32:100593. https://doi.org/10.1016/j.uclim.2020.100593

595 Sangha KK, Gordon IJ, Costanza R (2022) Ecosystem Services and Human Wellbeing-Based
596 Approaches Can Help Transform Our Economies. Frontiers in Ecology and Evolution
597 10:841215. https://doi.org/10.3389/fevo.2022.841215

598 Sekertekin A, Zadbagher E (2021) Simulation of future land surface temperature distribution and
599 evaluating surface urban heat island based on impervious surface area. Ecological Indicators
600 122:107230. https://doi.org/10.1016/j.ecolind.2020.107230

601 Shan W, Jin X, Ren J, Wang Y, Xu Z, Fan Y, Gu Z, Hong C, Lin J, Zhou Y (2019). Ecological
602 environment quality assessment based on remote sensing data for land consolidation. Journal
603 of Cleaner Production, 239, 118126. https://doi.org/10.1016/j.jclepro.2019.118126

604 Shelestov A, Lavreniuk M, Kussul N, Novikov A, Skakun S (2017) Exploring Google Earth
605 Engine Platform for Big Data Processing: Classification of Multi-Temporal Satellite
606 Imagery for Crop Mapping. Frontiers in Earth Science 5:17.
607 https://doi.org/10.3389/feart.2017.00017

608 Sobrino JA, Jiménez-Muñoz JC, Paolini L (2004) Land surface temperature retrieval from
609 LANDSAT TM 5. Remote Sensing of Environment 90(4):434–440.
610 https://doi.org/10.1016/j.rse.2004.02.003

611 Soma K, Hennen W, van Berkum S (2023) Can Domestic Food Production Provide Future Urban
612 Populations with Food and Nutrition Security? Insights from Bangladesh, Kenya and
613 Uganda. Sustainability 15(11):19005. https://doi.org/10.3390/su15119005

614 Su Y, Feng G, Ren J (2023) Spatio-temporal evolution of land use and its eco-environmental effects
615 in the Caohai National Nature Reserve of China. Scientific Reports 13(1):47471.
616 https://doi.org/10.1038/s41598-023-47471-4

617 Sun C, Li J, Liu Y, Cao L, Zheng J, Yang Z, Ye J, Li Y (2022) Ecological quality assessment and
618 monitoring using a time-series remote sensing-based ecological index (ts-RSEI). GIScience
619 and Remote Sensing 59(1):1793–1816. https://doi.org/10.1080/15481603.2022.2138010

620 Svoboda J, Štych P, Laštovička J, Paluba D, Kobliuk N (2022). Random Forest Classification of
621 Land Use, Land-Use Change and Forestry (LULUCF) Using Sentinel-2 Data—A Case Study
622 of Czechia. Remote Sensing, 14(5). https://doi.org/10.3390/rs14051189

623 Tikuye BG, Rusnak M, Manjunatha BR, Jose J (2023). Land Use and Land Cover Change
624 Detection Using the Random Forest Approach: The Case of The Upper Blue Nile River Basin,
625 Ethiopia. Global Challenges, 7(10), 1–11. https://doi.org/10.1002/gch2.202300155

626 Tolessa T, Senbeta F, Kidane M (2017) The impact of land use/land cover change on ecosystem
627 services in the central highlands of Ethiopia. Ecosystem Services 23:47–54.
628 https://doi.org/10.1016/j.ecoser.2016.11.010

629 Ullah N, Siddique MA, Ding M, Grigoryan S, Zhang T, Hu Y (2022) Spatiotemporal Impact of
630 Urbanization on Urban Heat Island and Urban Thermal Field Variance Index of Tianjin
631 City, China. Buildings 12(4):399. https://doi.org/10.3390/buildings12040399

632 Wang H, Liu C, Zang F, Liu Y, Chang Y, Huang G, Fu G, Zhao C, Liu X (2023) Remote Sensing-
633 Based Approach for the Assessing of Ecological Environmental Quality Variations Using
634 Google Earth Engine: A Case Study in the Qilian Mountains, Northwest China. Remote
635 Sensing 15(4):960. https://doi.org/10.3390/rs15040960

636 Wang X, Yao X, Jiang C, Duan W (2022) Dynamic monitoring and analysis of factors influencing
637 ecological environment quality in northern Anhui, China, based on the Google Earth
638 Engine. Scientific Reports 12(1):24413. https://doi.org/10.1038/s41598-022-24413-0

639 Wei X, Cheng T, Yang J, Qiao S, Li L, Yu H, Mi X, Liu Y, Guo H, Li J, Sun Y, Wang C, Gu X
640 (2023) Spatio-Temporal Changes in Ecosystem Quality across the Belt and Road Region.
641 Sensors 23(18). https://doi.org/10.3390/s23187752

642 Xu H, Wang Y, Guan H, Shi T, Hu X (2019). Detecting ecological changes with a remote sensing
643 based ecological index (RSEI) produced time series and change vector analysis. Remote
644 Sensing, 11(20), 1–24. https://doi.org/10.3390/rs11202345

645 Yang Z, Li W, Li X, Wang Q, He J (2019) Assessment of eco-geo-environment quality using
646 multivariate data: A case study in a coal mining area of Western China. Ecol Indic 107.
647 https://doi.org/10.1016/j.ecolind.2019.105651

648 Yin D, Li X, Li G, Zhang J, Yu H (2020) Spatio-temporal evolution of land use transition and its
649 eco-environmental effects: A case study of the Yellow River Basin, China. Land 9(12):1–25.
650 https://doi.org/10.3390/land9120514

651 Yuan B, Fu L, Zou Y, Zhang S, Chen X, Li F, Deng Z, Xie Y (2021) Spatiotemporal change
652 detection of ecological quality and the associated affecting factors in Dongting Lake Basin,
653 based on RSEI. J Clean Prod 302. https://doi.org/10.1016/j.jclepro.2021.126995

654 Yue H, Liu Y, Li Y, Lu Y (2019) Eco-environmental quality assessment in China's 35 major cities
655 based on remote sensing ecological index. IEEE Access 7:51295–51311.
656 https://doi.org/10.1109/ACCESS.2019.2911627

657 Zhang K, Feng R, Zhang Z, Deng C, Zhang H, Liu K (2022) Exploring the Driving Factors of
658 Remote Sensing Ecological Index Changes from the Perspective of Geospatial
659 Differentiation: A Case Study of the Weihe River Basin, China. Int J Environ Res Public
660 Health 19(17):1–25. https://doi.org/10.3390/ijerph191710930

661

662